

## Visualization of O<sub>2</sub> Partial Pressures in Running PEFC with Straight Channels

K. Nagase,<sup>a,b</sup> M. Uchida,<sup>a</sup> J. Inukai,<sup>a</sup>  
Y. Nagumo,<sup>c</sup> H. Motegi,<sup>d</sup> M. Yoneda,<sup>d</sup>  
T. Suga,<sup>e</sup> H. Nishide,<sup>e</sup> M. Watanabe<sup>a</sup>

<sup>a</sup>University of Yamanashi, Kofu, Japan, <sup>b</sup>TAKAHATA PRECISION JAPAN, Fuefuki, Japan, <sup>c</sup>Shimadzu Corporation, Kyoto, Japan, <sup>d</sup>Mizuho Information and Research Institute, Tokyo, Japan, <sup>e</sup>Waseda University, Tokyo, Japan

Practical use of PEFCs, including the transportation, is now pushed forward. For the efficient design of cells as well as MEAs, it is important to understand the reactions inside the cells in real time and space during the power generation. For this purpose, we have developed a new visualization method for oxygen<sup>1</sup> and carbon dioxide<sup>2</sup> inside PEFCs; cells with a transparent window and a dye sensitive to oxygen or carbon dioxide have been used. In all the studies, the flow channels have been of a serpentine-type. For automobiles, for example, straight-type flow channels are mainly used in PEFCs, and efficiency of the development is demanded. Moreover, simple straight flow channels are suitable for analyzing a PEFC as a system with the combination of a numeric simulation,<sup>3</sup> which helps us to understand the fundamental processes of power generation. Therefore, the visualization of a PEFC with straight channels has been desired. The data thus-obtained should be useful as the basic information for the development of efficient PEFCs with a uniform distribution of power generation as well as for the optimal operation conditions. In this study, we analyzed reactions in a cell with straight channels by observing the O<sub>2</sub> partial pressure ( $p_{O_2}$ ) on the GDL at the cathode during the power generation.



Fig. 1 See-Through PEFC with straight flow channels at the cathode.

Figure 1 shows a see-through PEFC with five straight parallel channels, 54 mm in length, 1 mm in width, 0.6 mm in depth with pitches of 1 mm. A transparent cathode endplate is made of quartz glass, carefully chosen and manufactured to have high transparency, low refractivity, and high thermal conductivity. The MEA surface is coated with PtPP (tetrakis (pentafluorophenyl) porphyrinato platinum), a dye sensitive to oxygen. Using the cell, the visualization inside the cell was realized by obtaining the intensity of luminescence emitted from the dye during the irradiation of laser light. The luminescence was captured by a CCD camera in a dark room.

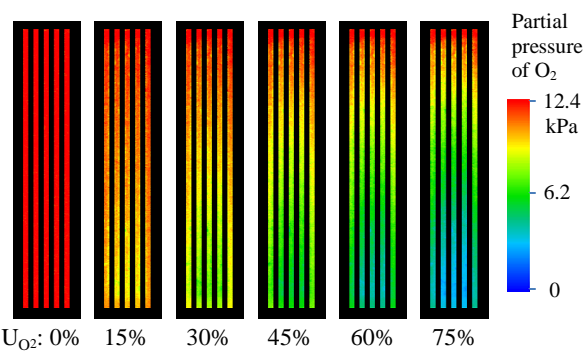


Fig. 2  $p_{O_2}$  on the GDL surface visualized in an operating PEFC. Cell temperature = 80 °C; relative humidity = 80% (H<sub>2</sub> and air); H<sub>2</sub> flow rate = 200 ml min<sup>-1</sup>; current density = 0.6 A cm<sup>-2</sup>; U<sub>O<sub>2</sub></sub> = 0, 15, 30, 45, 60, 75%; holding time on each condition = 5 min.

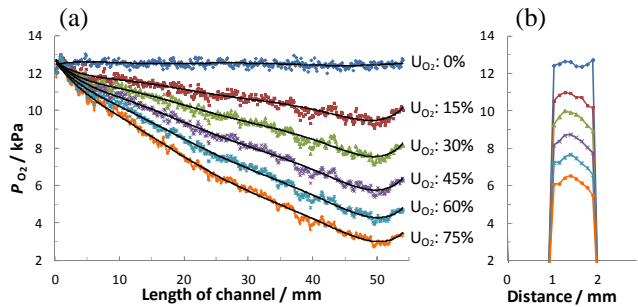


Fig. 3  $p_{O_2}$  along the center channel (a) and along the horizontal line in the middle of the center channel (b) at 0.6 A cm<sup>-2</sup>.

Prior to the power generation, the calibration curves, known as Stern-Volmer plots, of the dye film were obtained under the mixed gases of O<sub>2</sub> and N<sub>2</sub> (O<sub>2</sub> concentration = 2 to 25%). The gas in the cell was fully purged, and the cell operation was started at the cell temperature of 80 °C with humidified air and H<sub>2</sub>. During the operation, the light emission from the GDL surface was captured by a CCD camera. The spatial resolution was 120  $\mu$ m. Images for the emissions were converted to  $p_{O_2}$  images using the Stern-Volmer plots. Figure 2 shows the distribution of  $p_{O_2}$  at the cathode during the cell operation. To examine the visualized images in detail,  $p_{O_2}$  was plotted along the center channel from the inlet to the outlet at different oxygen utilization (U<sub>O<sub>2</sub></sub>) in Fig. 3 (a), whereas  $p_{O_2}$  along the line perpendicular to the channel at the middle of it in Fig. 3 (b). At low U<sub>O<sub>2</sub></sub>,  $p_{O_2}$  on the GDL surface decreases linearly along the channel. As U<sub>O<sub>2</sub></sub> increases,  $p_{O_2}$  decreases more in the former half of the channel than in the latter half. As seen in Fig. 3(b),  $p_{O_2}$  was lower near the rib than in the middle of the channel, indicating low  $p_{O_2}$  under the ribs. Numerical analysis is now in progress to explain these  $p_{O_2}$  distributions.

### References

- 1) J. Inukai, et al., *Angew. Chem. Int. Ed.*, 120, 2834 (2008).
- 2) Y. Ishigami, et al., *Electrochim. Solid-State Lett.*, 15, B51 (2012).
- 3) M. Takimoto, et al., *J. Jpn. Soc. Appl. Electromagn. Mech.*, 14, 262 (2006).